Trajectory Planning for Multiple UAVs in UAV-aided Wireless Relay Network

Jongyul Lee and Vasilis Friderikos
Centre for Telecommunications Research, Department of Engineering
King's College London, London WC2R 2LS, U.K.
E-mail:{jongyul.lee, vasilis.friderikos}@kcl.ac.uk

ICC 2022 - IEEE International Conference on Communications | 978-1-5386-8347-7/22/$31.00 ©2022 IEEE | DOI: 10.1109/ICC45855.2022.9839010

***Abstract*—The integration of Unmanned Aerial Vehicle (UAV) as flying base station (FBS) assisted wireless communications has recently attracted significant attention. However, there is a need for efficient optimization trajectory techniques to allow for continuous service connectivity for FBSs operating at regions beyond single-hop backhauling to their depot (i.e., fixed macro base station). This work proposes an optimization trajectory planning framework to provide continuous service delivery of FBSs by utilizing aerial relay nodes which can also serve ground users (GUs). The proposed joint optimization framework of FBSs trajectories where a subset of them acts as relay nodes called relay-FBS (rFBS) provides tangible gains compared to previously proposed nominal techniques. More specifically, a wide set of numerical investigations reveals that the proposed framework reduces aggregate travel time (ATT) more than 14% for the entire fleet of FBSs, whilst for rFBS to enable continuous service support, this average gain is more than 38%.**

***Index Terms*—Mixed Integer Linear Programming (MILP), Unmanned Aerial Vehicle (UAV), UAV Relay network, Wireless Networks, B5G, Path Planning, Flying Base Station (FBS).**

I. Introduction

RECENTLY Unmanned Aerial Vehicles (UAVs) acting as flying base stations (FBSs)[1] have received remarkable research attention in assisting wireless networks due to their significant potential of versatility, high and flexible mobility, computational performance, and high probability of line of sight (LoS) transmission compared with other conventional means, rendering them substantially useful and valuable for the case of Internet of Things (IoT) applications, surveillance for military and emergency disasters [1] to name just a few. However, in several instances when serving ground users (GUs), FBSs might need to operate beyond their single-hop bachauling range to a terrestrial BS (depot). In that case, a relay FBS, which is also serving GUs, is required to maintain real-time communications. This specific problem of provisioning real-time communications using relay-FBSs has not been thoroughly investigated and this work tries to fill this void by detailing a joint optimization trajectory design for FBSs that require a relay FBS. With limited capacity of on-board batteries, UAVs have restricted available flying time since they in both flying or hovering mode [2]. Hence, creating an efficiently cooperative trajectory for the multiple UAVs allows not only to reduce the travel time, an aspect of which is relates to the energy consumption, but also to increase the flying frequency over an area of interest (AoI). Therefore, the above aspects can be deemed as being crucial in designing effective UAV-aided beyond 5G (B5G) networks. Due to the plethora of potential applications of UAVs serving as FBSs as aforementioned, the underlying trajectory optimization of FBSs in the UAV relay network system has recently attracted substantial levels of interest [1], [3]–[12]. Particularly, the works in [3], [4], [6], [8]–[12] address the power control of the UAV such as transmit power in constructing the UAV trajectory. What's more, the focus of references [4]–[9] is on maximizing throughput in order to improve the network capacity of the system. For further improvement on the UAV relay network system performance, the works in [10]–[12] introduce the energy efficiency for the operation of the UAV.

To the best of our knowledge, there are no other works that consider an energy efficient trajectory design for multiple UAVs for a large distributed area in a UAV relay network. One of the major challenges in UAV deployment is to design the trajectory to prolong the UAV's operation time including its service. Hence, this is vital for multiple UAVs to efficiently deploy such the highly spatially distributed relay network. In addition, since the UAV's on-board energy is considerably limited, they require a terrestrial macro-cellular BS acting as a depot where UAVs are dispatched and return, i.e., Hamiltonian paths for UAVs. This provides the necessary mechanism for the FBS to recharge in order to continue their mission iterations.

Furthermore, for a UAV relay network in a practical real-world situation, it is important to deploy multiple UAVs to ensure continuous communication to a terrestrial BS via multi-hop communication. However, the works in [1], [3], [6], [7], [9], [10] did not consider an multiple UAVs operation, whilst the ones in [3], [5]–[7], [9], [10] did not take into account an multi-hop framework. Moreover, the works in [1], [3], [11] only considered stationary UAVs whilst the UAVs are required for motion planning in practical approach. Also, the references in [11], [12] are not taking into consideration the energy consumption for the UAV trajectory in an explicit manner. These motivate us to propose a new framework to solve a problem of the UAV trajectory planning design for energy minimization in a UAV relay network scenario. To overcome the limitation in the prior works above mentioned, we design a Hamiltonian path-based energy efficient UAV-enabled trajectory planning for multiple UAVs with multi-hop deployed in practical scenario such as the large distributed area.

The key novelties and contributions of this work are as follows. We formulate a multiple UAVs hosted on a macro-

[1]Hereafter, the terms of 'UAV' and 'FBS' are used interchangeably.

BS trajectory planning optimization problem for wireless relay deployment using a mixed integer linear programming (MILP) model, i.e., a Hamiltonian path-based trajectory planning formulation. The proposed formulation provides a novel UAV relay network system. It is composed of two types of UAVs: i) a UAV that directly serves GUs at the end point, which is also called FBS, ii) an assistant UAV called relaying FBS (rFBS) that assists the FBS for relay to forward packets collected from the GUs to the macro-BS. The rFBS is only operated in the case that the FBS attempts to serve GUs in a remote area where the terrestrial BS cannot communicate via direct single hop communication. Furthermore, an energy efficient UAVs trajectory planning is proposed for the relay deployment to reduce the total consuming energy for FBSs by minimizing their aggregate travel time (ATT). To tackle the inherent NP-hardness of the problem [13], a competitive heuristic algorithm is presented. Finally, a wide set of numerical investigations reveals the potential gains of the proposed schemes compared to the state of art.

II. System Model

The underlying scenario of the UAV-assisted B5G relay network is depicted in Fig. 1. A B5G terrestrial macro BS is located in the center of a cell. A set of FBSs; multiple UAVs including a set of serving FBSs and relay FBSs (rFBSs) are allocated at the macro BS which acts as a depot for those FBSs. Moreover, the macro BS is aware regarding information about clusters who need to improve the network performance. A set of cluster points (CPs) are randomly distributed within a pre-defined geographical area in the cell wireless network. A CP is defined as the center of a cluster of GUs that needs to send/receive packets for communication. The CPs are taxonomized into two parts: i) A CP out of the cell coverage (CP$_{out}$) and ii) a CP in the cell coverage (CP$_{in}$). The CP$_{out}$ requires a relay UAV in addition to the serving UAV to ensure service continuity, whilst the CP$_{in}$ does not require a relay node for communicating to the BS via a serving UAV. All the FBSs (FBS and rFBS) are dispatched and return to the original depot (the macro-BS) to replenish their battery/fuel. A single FBS only serves at each CP in order to avoid duplicate service and begins to serve GUs whilst hovering once arriving at a specific CP. All FBSs equally serve requested data for those GUs. The FBS involved in the service hovers over the GUs and at the same time the rFBS hovers on the relay position (RP) in order to relay and transmit data from/to the GUs. Once the service is completed at a CP, the FBS moves to the next CP and the rFBS follows the FBS for the relay. If the FBS visits all assigned CPs, it returns to the depot. Meanwhile, the rFBS returns to the BS once all the relay for services at CP$_{out}$s are completed. A rFBS arrives on time at a RP feasible to relay for a serving FBS. Without loss of generality, the RP of an rFBS is assumed to be located on the middle of the Euclidean distance between the BS and the location of FBS serving at the CP$_{out}$.

A. Network Model

Without loss of generality, we assume that all FBSs hover with constant velocity and at the same altitude when they are operated in the network. With that in mind, the aforementioned scenario in the UAV-assisted B5G relay network is modeled as an undirected graph $\mathcal{G} = (\mathcal{V}, \mathcal{E})$, where $\mathcal{V}$=$\{1, 2, \cdots, N_V\}$ denotes a set of nodes, the elements of which are included in a two dimensional Cartesian coordinate system, i.e., the horizontal plane, $\mathbb{R}^{2\times 1}$. $\mathcal{E}$=$\{(i,j) : i,j \in \mathcal{V}, i \neq j\}$ is a set of links (routes) which are defined as d_{ij}, i.e., the Euclidean distance. $\mathcal{V} = \mathcal{N} \cup \mathcal{S}_r$, where $\mathcal{N}$ denotes a set of CPs. $\mathcal{N} = \mathcal{N}_{out} \cup \mathcal{N}_{in}$, where $\mathcal{N}_{out}$=$\{1, 2, \cdots, N_{out}\}$ represents a set of CP$_{out}$s and $\mathcal{N}_{in}$=$\{1, 2, \cdots, N_{in}\}$ represents a set of CP$_{in}$s. Also, $\mathcal{S}_r$=$\{1, 2, \cdots, S_R\}$ denotes a set of RPs and it is worth noticing $|\mathcal{N}_{out}|$=$|\mathcal{S}_r|$, where $|.|$ is defined as the cardinality of the set. For purposes of notational convenience, an extended notation $\mathcal{V}_+$=$\mathcal{V} \cup \{0\}$ is used in which the index 0 represents the macro BS, whilst $\mathcal{N}_+$ and $\mathcal{S}_{r+}$ are as defined above. Moreover, the set of FBSs is denoted by $\mathcal{K}$=$\{1, 2, \cdots, N_K\}$ and the set of rFBSs is defined by $\mathcal{U}$=$\{1, 2, \cdots, N_U\}$. Let $\mathcal{B} = \{1, 2, \cdots, N_B\}$ be the set of GUs. The horizontal location of the GU $b \in \mathcal{B}$ is denoted as $\mathbf{w}_b \in \mathbb{R}^{2\times 1}$. v_k and v_u are denoted as the velocity of FBS k, $k \in \mathcal{K}$ and rFBS u, $u \in \mathcal{U}$, respectively, and let H be the altitude of the FBS.

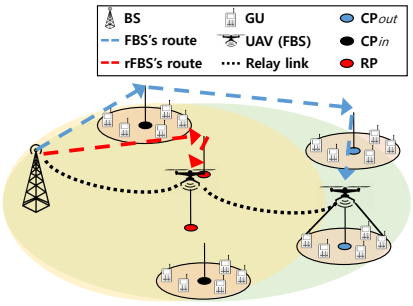

Fig. 1. An overview of the UAV-aided relay network system.

B. Transmission Model

We assume a downlink scenario. The FBS flies at a constant altitude H in meters and hence the distance between the FBS and GU b at CP i is given by,

$$\mathbf{d}_{b,i} = \sqrt{H^2 + ||\mathbf{q}_k - \mathbf{w}_{b,i}||^2}, \tag{1}$$

where $\mathbf{q}_k \in \mathbb{R}^{2\times 1}$ denotes the FBS trajectory projected onto the horizontal plane, i.e., the location of CP i. In this paper, since we are interested in the average signal strength rather than the instantaneous one, we only consider the effects of the Line of Sight (LoS) and none-LoS (NLoS) link impairments for the air to ground link [14], [15]. The work in [14] modelled the LoS connection probability between the FBS and the GU b at CP i denoted as $\mathbb{P}_{b,i,\text{LoS}}$ as follows,

$$\mathbb{P}_{b,i,\text{LoS}} = \frac{1}{1 + C\ \exp(-D[\theta_{b,i} - C])}, \tag{2}$$

where C and D are constant values which depend on the propagation environment, e,g,. rural, urban, dense urban, etc. $\theta_{b,i} = \frac{180}{\pi}\sin^{-1}(H/\mathbf{d}_{b,i})$ is the elevation angle in degree.

Worths clearly interesting that the LoS probability $\mathbb{P}_{b,i,\text{LoS}}$ is dependent on the FBS trajectory $\mathbf{q}_k$. Furthermore, the regularized LoS probability by considering the effect of NLoS occurrence with the attenuation factor η is represented as given by [16],

$$\hat{\mathbb{P}}_{b,i,\text{LoS}} = \mathbb{P}_{b,i,\text{LoS}} + (1 - \mathbb{P}_{b,i,\text{LoS}})\eta. \tag{3}$$

Let P_t denote the transmit power of the FBS when a GU is scheduled for the service. The achievable throughput rate $R_{b,i}$ in bits per second (bps) between the UAV and the GU b at CP i is represented as,

$$R_{b,i} = B\log_2\left(1 + \frac{\gamma_0 \hat{\mathbb{P}}_{b,i,\text{LoS}}}{(H^2 + ||\mathbf{q}_k - \mathbf{w}_{b,i}||^2)^{\alpha/2}}\right), \tag{4}$$

where $\gamma_0 \triangleq P_t\beta_0/(\sigma_0\Gamma)$ in which β_0 is the pass loss at the reference distance, σ_0 is the noise power at the receiver, and Γ is a constant accounting for the gap from the channel capacity. Also, α denotes a path loss exponent [16]. The constant values used in Eqs. (2)−(4) are referred for further details in Table I. Let $Q_{b,i}$ denote the length of the requested data in bits for GU b at CP i and therefore the service (the required transmission) time denoted as $s_{b,i}$ is computed by $s_{b,i} = Q_{b,i}/R_{b,i}$.

C. Energy Consumption Model for rotary wings of a UAV

In this paper, we adopt a UAV controlled with rotary wings. Hence, a widely-used energy consumption model is applied and plugged into the proposed framework. The propulsion power consumption caused by the flying velocity in watts (W) can be approximately expressed as follows [16],

$$\begin{aligned} P_T =& P_0\left(1 + \frac{3v^2}{U_{tip}^2}\right) + P_I\left(\sqrt{1 + \frac{v^4}{4V_0^4}} - \frac{v^2}{2V_0^2}\right)^{1/2} \\ &+ \frac{1}{2}\xi_0\rho\hat{s}Av^3, \end{aligned} \tag{5}$$

where v in m/s is the velocity of the FBS. The other constant parameters in Eqs. (5) are referred for further details in Table I. We consider two types of UAV energy propulsion consumption; traveling and hovering mode energy consumption. Specifically, P_T as expressed in Eqs. (5) denotes the traveling mode energy by defining the energy required to travel between different nodes. The hovering mode energy is defined as the energy when an FBS hovers over a CP or a RP to serve GUs or relay. This is simply represented as $\hat{P}_H$ by inserting $v = 0$ into Eqs. (5), which in that case can be written as $\hat{P}_H = P_0 + P_I$. Also, since the FBS serves GUs only when hovering at a CP, we can define the hovering mode of energy consumption of the FBS as P_H with defining the communication-related power as P_c as $P_H = \hat{P}_H + P_c$.

III. Problem Formulation and Heuristic Algorithm

A. UAV Relay Trajectory Planning Formulation

In this section, based on the discussed scenario and aforementioned system model, we provide a proposed MILP formulation for path planning optimization with FBSs, which aims to minimize the aggregate FBSs flying time.

To start with, two decision variables for the FBS of the proposed model can be defined as follows. The decision variable x_{ijk} is equal to 1 if an FBS k uses a link (route) between a node[2] i and a node j, otherwise 0. Also, the decision variable w_{ik} is continuous variable greater zero, meaning arrival time at which service begins at a CP i by an FBS k. We then derive several constraints to create an FBS trajectory and time window in the relay network as follows,

$$\sum_{\substack{i\in\mathcal{N}_+\\(i\neq j)}}\sum_{k\in\mathcal{K}} x_{ijk} = 1, \quad \forall j \in \mathcal{N}_+, \tag{6a}$$

$$\sum_{\substack{j\in\mathcal{N}_+\\(i\neq j)}} x_{jik} = \sum_{\substack{j\in\mathcal{N}_+\\(i\neq j)}} x_{ijk}, \quad \forall k \in \mathcal{K}, \quad \forall i \in \mathcal{N}_+, \tag{6b}$$

The constraints in (6a) and (6b) create an FBS trajectory. The constraint in (6a) allows that an FBS k travels from a node i to a node j. The constraint in (6b) guarantees that an FBS k departs and arrives at a determined node. Observe that this set of constraints also ensures flow conservation of the FBS route.

$$e_{0k} + t_{0jk} \leq w_{jk} + \lambda(1 - x_{0jk}), \quad \forall k \in \mathcal{K}, \quad \forall j \in \mathcal{N}, \tag{7a}$$

$$w_{ik} + s_{b,i} + t_{ijk} \leq w_{jk} + \lambda(1 - x_{ijk}), \forall k \in \mathcal{K}, \forall i, j(i \neq j) \in \mathcal{N}, \tag{7b}$$

$$w_{ik} + s_{b,i} + t_{i0k} \leq x_{i0k}(l_{0k} - \lambda) + \lambda, \quad \forall k \in \mathcal{K}, \quad \forall i \in \mathcal{N}, \tag{7c}$$

$$w_{jk} \leq e_{0k} + t_{0jk} + \lambda(1 - x_{0jk}), \quad \forall k \in \mathcal{K}, \quad \forall j \in \mathcal{N}, \tag{7d}$$

$$w_{jk} \leq w_{ik} + s_{b,i} + t_{ijk} + \lambda(1 - x_{ijk}), \forall k \in \mathcal{K}, \forall i, j(i \neq j) \in \mathcal{N}. \tag{7e}$$

$$e_{ik} \leq w_{ik} \leq l_{ik}, \quad \forall k \in \mathcal{K}, \ \forall i \in \mathcal{N}. \tag{7f}$$

The constraints in (7a)−(7f) represent the time window for the FBS trajectory. We note that λ is a sufficiently large constant. The constraint in (7a) represents the earliest time where an FBS k can start being deployed; e_{0k} is the mission start time of the FBS k at the BS; t_{0jk} denotes the traveling time of an FBS k between nodes, i.e., $t_{0j} = d_{0j}/v_k$. The constraint in (7b) ensures that an FBS k arrives and begins to serve at a CP j after the FBS k serves during the service time s for GU b and then travels from a CP i. The constraint in (7c) ensures that an FBS k returns to the BS before the maximum window time l_{0k}. The constraints in (7d)−(7e) allow to validate the precise arrival time of FBS k at each CP. The constraint in (7f) guarantees that an FBS k serves GUs at CP i within the time window, i.e., QoS support.

Furthermore, we also define three additional decision variables for the rFBS as follows. The decision variable y_{iju} is equal to 1 if an rFBS u uses a link (route) between a node i and a node j, otherwise 0. The decision variable q_{iu} is continuous variable greater zero meaning that arrival time for an rFBS u at a RP i and the decision variable z_{iju} is continuous variable greater zero meaning that travel time of an rFBS u between a

[2]The word 'node' is used to include the notations of 'BS', 'CP' and 'RP'.

node i and a node j. We then provide constants to create an rFBS trajectory with time window as follows,

$$\sum_{\substack{i\in\mathcal{S}_+\\(i\neq j)}}\sum_{u\in\mathcal{U}} y_{iju}=1,\quad \forall j\in\mathcal{S}_{r+}, \tag{8a}$$

$$\sum_{\substack{j\in\mathcal{S}_+\\(i\neq j)}} y_{jiu}=\sum_{\substack{j\in\mathcal{S}_+\\(i\neq j)}} y_{iju},\quad \forall u\in\mathcal{U},\quad \forall i\in\mathcal{S}_{r+}, \tag{8b}$$

$$w_{ik}=q_{ju},\ \forall i\in\mathcal{N}_{out},\ \forall j\in\mathcal{S}_r,\ \forall k\in\mathcal{K},\ \forall u\in\mathcal{U}, \tag{8c}$$

$$q_{iu}+z_{iju}\leq q_{ju}+\lambda(1-y_{iju}),\ \forall u\in\mathcal{U},\quad \forall i,j(i\neq j)\in\mathcal{S}_r, \tag{8d}$$

$$q_{ju}\leq q_{iu}+z_{iju}+\lambda(1-y_{iju}),\ \forall u\in\mathcal{U},\quad \forall i,j(i\neq j)\in\mathcal{S}_r, \tag{8e}$$

$$z_{0iu}=d_{0i}/v_u,\quad \forall u\in\mathcal{U},\quad \forall i\in\mathcal{S}_r, \tag{8f}$$

$$z_{i0u}=d_{i0}/v_u,\quad \forall u\in\mathcal{U},\quad \forall i\in\mathcal{S}_r, \tag{8g}$$

The constraints in (8a) and (8b) create an rFBS trajectory. The constraint in (8c) guarantees that arrival time of both an FBS k at a CP$_{out}$ and an rFBS u at a RP is identical so that the pair of FBSs starts the service on the required starting point of the time window. The constraint in (8d) constructs the time window for an rFBS u and the constraint in (8e) enables the precise and valid arrival time to be obtained. The constraints in (8f) and (8g) represent the initial and final travel time of an rFBS u from/to the BS.

Based on the above specific constraints, the MILP model for the FBSs relay trajectory planning optimization with time window can be formulated as follows,

$$\text{(P1):}\quad \min_{\substack{\{q_{iu}\},\{w_{ik}\},\\ \{x_{ijk}\},\{y_{iju}\},\{z_{iju}\}}} \sum_{k\in\mathcal{K}}\sum_{i\in\mathcal{N}_+}\sum_{\substack{j\in\mathcal{N}_+\\(i\neq j)}} t_{ijk}x_{ijk} \tag{9}$$

$$\text{s. t.}\quad \text{(6a), (6b), (7a)}-\text{(7f), (8a)}-\text{(8g),}$$

$$x_{ijk}\in\{0,1\},\quad \forall k\in\mathcal{K},\quad \forall i,j(i\neq j)\in\mathcal{N}_+, \tag{10}$$

$$y_{iju}\in\{0,1\},\quad \forall u\in\mathcal{U},\quad \forall i,j(i\neq j)\in\mathcal{S}_{r+}, \tag{11}$$

$$w_{ik}\geq 0,\quad \forall k\in\mathcal{K},\quad \forall i\in\mathcal{N}, \tag{12}$$

$$q_{iu}\geq 0,\quad \forall u\in\mathcal{U},\quad \forall i\in\mathcal{S}_r, \tag{13}$$

$$z_{iju}\geq 0,\quad \forall u\in\mathcal{U},\quad \forall i,j(i\neq j)\in\mathcal{S}_r. \tag{14}$$

The constraints in (10) and (11) represent that the decision variable x and y are binary. Also, the constraints in (12)$-$(14) represent that the decision variable w, q and z are continuous as well as greater than zero.

B. Energy Efficient UAV Relay Trajectory Formulation

The problem (P1) optimizes FBSs trajectories planning and finds the best trajectories planning that contains a Hamiltonian path, which resembles a TSP-based scheme [17]. However, the rFBS trajectory in the problem (P1) is not globally optimized in terms of ATT, which may consume a large amount of energy of the rFBS. Therefore, in this section, we propose an energy efficient UAV relay trajectory planning called (P2), as follows,

$$\text{(P2):}\quad \min_{\substack{\{q_{iu}\},\{w_{ik}\},\\ \{x_{ijk}\},\{y_{iju}\},\\ \{z_{iju}\}}} \sum_{k\in\mathcal{K}}\sum_{i\in\mathcal{N}_+}\sum_{\substack{j\in\mathcal{N}_+\\(i\neq j)}} t_{ijk}x_{ijk}+\sum_{u\in\mathcal{U}}\sum_{i\in\mathcal{S}_{r+}}\sum_{\substack{j\in\mathcal{S}_{r+}\\(i\neq j)}} z_{iju} \tag{15}$$

$$\text{s. t.}\quad \text{(6a), (6b), (7f)}-\text{(7e), (8a)}-\text{(8g), (10)}-\text{(14).}$$

Thus, the problem (P2) is to construct FBSs trajectories with the time windows for the wireless UAV relay network with the goal minimizing the ATT for both the FBS and the rFBS.

C. Proposed Heuristic Algorithm

Finding optimal trajectory suffers from the curse of dimensionality problem since the complexity of the underlying mathematical programs resembles the well-known TSP and VRP, which are both known to be NP-hard [13]. In this section, we present a local search heuristic algorithm as a high-quality approximate solution with polynomial complexity, which is also called Local Search for Energy Efficient Trajectory (LS-EET). It is designed for the UAV relay network to find competitive solutions to the UAV trajectory problem. The pseudo code of the algorithm is summarized in Alg. 1.

The proposed LS-EET creates both trajectories at the beginning of the algorithm, which solves the problem (P2) in a similar manner. Moreover, the trajectories created in the LS-EET are composed of string indices in which there are nodes that the FBS will visit, i.e., the number included in $\mathcal{V}_+$. The detail of this mechanism can be seen in the reference [18]. The goal of the LS-EET is to improve the total cost in order to find competitive routes for both FBS and rFBS. Hence, to mix the string-based trajectories in an advanced way, we propose a method which is in essence inspired by the well-known local search technique (LST), i.e., 2-Opt, Relocate, Swap [19], [20]. In the For loop from Step 6 to Step 17 in Alg. 1, one of these techniques is randomly selected to mix the string-based FBSs routes (trajectories) so that the LS-EET finds a better cost. Then, the entire process is repeated iteratively and the best feasible FBSs trajectories are selected in a greedy manner.

IV. Numerical Investigations

In this section a wide set of numerical investigations are presented to shed light on the effectiveness of the proposed schemes. Table I encapsulates the parameters used for performance evaluation. We set the AoI as a cell area (C_{aoi}) that has shape of a quarter of circle and its radius is set to 600 m. We randomly allocate CP$_{out}$s and CP$_{in}$s outside/inside of the C_{aoi}. The number of CP$_{out}$s (N_{out}) and CP$_{in}$s (N_{in}) is varied and for a fair comparison, the number of both FBSs (K) and rFBSs (U) is fixed to one. We assume that GUs are located at the mid-center of the CP. Without loss of generality, the velocity of v_k and v_u are fixed to 10.21 m/s that consumes the minimum energy of the FBS with the maximum endurance [16]. However, worth pointing out that when the rFBS travels between RPs, the velocity of the rFBS is differed from the fixed velocity of the rFBS since the rFBS's movement depends on the FBS

Algorithm 1 Local Search for Energy Efficient Trajectory (LS-EET)

I_{t}, $\Theta \leftarrow$ Initialize iteration number, parameters in Table I
$\mathcal{K}$, $\mathcal{U}$, $\mathcal{V}_+ \leftarrow$ Generate an FBS (K), an rFBS (U), CP$_{out}$s (N_{out}), RPs (S_R), CP$_{in}$s (N_{in}) and a BS (0).
$R_H(\mathcal{K}, \mathcal{V}_+, \Theta) \leftarrow$ Generate FBS trajectory by inserting CP$_{out}$s, CP$_{in}$s and a BS into string indices in K rows in a random distributed manner by solving Eqs. (6a), (6b), (7a)−(7f).
$R_R(\mathcal{U}, R_H) \leftarrow$ Generate rFBS trajectory by inserting RPs, CP$_{out}$s and the BS into string indices in U rows by solving Eqs. (8a)−(8f).
$\Delta \leftarrow$ Compute a total time cost of $\{R_H(\mathcal{K}, \mathcal{V}_+, \Theta) + R_R(\mathcal{U}, R_H)\}$.
for $T \coloneqq 0$ to I_t **do**
  $\Gamma \leftarrow$ Select LST randomly. // 2-Opt, Relocate, Swap [19], [20].
  $R'_H(\mathcal{K}, \mathcal{V}_+, \Theta, \Gamma) \leftarrow$ Execute the LST and update the string indices.
  $R'_R(\mathcal{U}, R_H) \leftarrow$ Update the string indices.
  $\Delta' \leftarrow$ Compute a new time cost of $\{R'_H(\mathcal{K}, \mathcal{V}_+, \Theta) + R'_R(\mathcal{U}, R'_H)\}$.
  if $\Delta' < \Delta$ **then**
    $R_H(\mathcal{K}, \mathcal{V}_+, \Theta, \Gamma) \leftarrow R'_H(\mathcal{K}, \mathcal{V}_+, \Theta, \Gamma)$
    $R_R(\mathcal{U}, R_H) \leftarrow R'_R(\mathcal{U}, R'_H)$
    $\Delta \leftarrow \Delta'$
  end if
  $I_t \leftarrow I_t - 1$
end for
return R_H, R_R, Δ; // Outcomes of FBS and rFBS trajectory, ATT$_k$, ATT$_u$ and ATT.

TABLE I
SIMULATION PARAMETERS.

Parameter	Value
Cell area (C_{aoi})	A quarter of circle
Cell radius (C_r)	600m
Location of BS	(0,0)(central)
Location of CP$_{in}$s	600m to 800m in C_{aoi}
Location of CP$_{out}$s	800m to 1000m in C_{aoi}
Allocation method for CPs	random distribution
Number of FBSs (K), rFBSs (U)	1, 1
Number of CP$_{out}$s (N_{out}), CP$_{in}$s (N_{in})	[2, 5], [4, 10]
Mission start/maximum time (e_0, l_0)	0, 5000 s
Velocity of FBS, rFBS (v_k, v_u)	10.21 m/s, 10.21 m/s [16]
Requested data (Q)	400 Kbits
Altitude of FBS (H)	100 m
Total communication bandwidth (B)	1 MHz
Iteration number (I_{t})	1500
γ_0, C, D, η, α, ξ_0	52.5 dB, 10, 0.6, 0.2, 2.3, 0.6 [16]
U_{tip}, V_0, A, ρ, $\hat{s}$	120, 4.03, 0.503, 1.225, 0.05 [16]
P_0, P_I, P_c	79.86 W, 88.63 W, 5 W [16]

serving at CP$_{out}$s. To intuitively observe the performance of our design, we assume that all GUs at each CP have identical average throughput requirements, i.e., $Q \triangleq Q_i = Q_{b,i}$. Then, Q is fixed to 400 Kbits. Furthermore, we compare performance of the following schemes incorporating baselines,

1) *(P1):* Trajectory planning optimized by the problem (P1) which is the typical TSP-based reference scheme in [17].
2) *(P2):* Trajectory planning optimized by the problem (P2).
3) *Energy Minimization (EM):* Trajectory planning optimized by the energy consumption minimization for a UAV controlled by the rotary wings modeled by Eqs. (5), which is a reference scheme in [10].
4) *LS-EET:* A heuristic trajectory planning algorithm applying the LST provided in the section III-C with Alg. 1.

Fig. 2 show an example of timelines and a trajectory of FBSs respectively for all schemes in the case when $N_V = 12$, and $Q = 400$ Kbits, i.e, $N_{out} = 3$, $N_{in} = 6$ and $S_R = 3$. The number 1 to 3 represents CP$_{out}$s and the number 4 to 9 denotes CP$_{in}$s whilst the number $1'$ to $3'$ represents RPs in Fig. 2. The black arrows indicate the direction of FBSs in Fig. 2. Worth

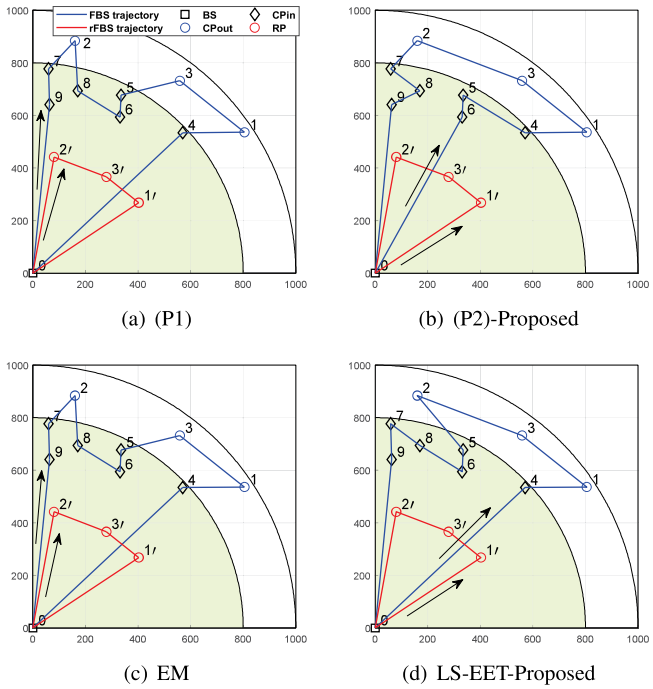

(a) (P1) (b) (P2)-Proposed

(c) EM (d) LS-EET-Proposed

Fig. 2. An example of the FBS trajectory for comparison with all different schemes when $N_{out} = 3$, $N_{in} = 6$, and $Q = 400$ Kbits. (a) ATT$_k$=1997s, ATT$_u$=1329s, (b) ATT$_k$=2004s, ATT$_u$=711s, (c) ATT$_k$=1997s, ATT$_u$=1329s, (d) ATT$_k$=2015s, ATT$_u$=711s.

observing that all schemes show different FBSs trajectories and different departure time of the rFBS, while the (P1) and the EM schemes illustrate the identical FBSs trajectories. Moreover, the (P1) and the EM schemes obtain the lowest ATT$_k$[3] at 1997s compared with other different schemes as shown in Fig. 2. However, these schemes gain the highest ATT$_u$ (which was 1329s) since the rFBS moves from the RP number $2'$ to $3'$ and waits until the FBS completes the service between the number 2 and 3, i.e., CP$_{out}$s. In other words, the FBS visits the CP number 2-8-6-5-3 in sequence and the rFBS does not support the number 8, 6 and 5. i.e., CP$_{in}$s. Whereas, both the (P2) and the LS-EET gain the ATT$_u$ at 711s respectively, whilst their departure times are different. Moreover, the (P2) and the LS-EET gain the ATT$_k$ at 2004s and 2015s respectively, which are almost identical compare with the ATT$_k$ (1997s) of the (P1) and the EM. That is, the FBS of the (P2) and the LS-EET visit the CP number 3-2 in sequence, i.e., CP$_{out}$ 3 and 2, which does not obviously visit any CP$_{in}$s between the CP$_{out}$ 3 and 2, while the rFBS moves from the RP number $3'$ to $2'$. Hence, the (P2) and the LS-EET schemes decrease the ATT$_u$ by 618s compared to the (P1) and the EM schemes.

Fig. 3(a) and (b) show the ATT including both the FBS and the rFBS for all different schemes, and the ATT$_k$ and the ATT$_u$ respectively for all different schemes. We varied N_V including N_{out} and N_{in} in ratio of 1:2. In Fig. 3(a),

[3]We note that ATT$_k$ and ATT$_u$ represent ATT of the FBS and the rFBS respectively, while ATT represents ATT of the entire fleet of the FBSs.

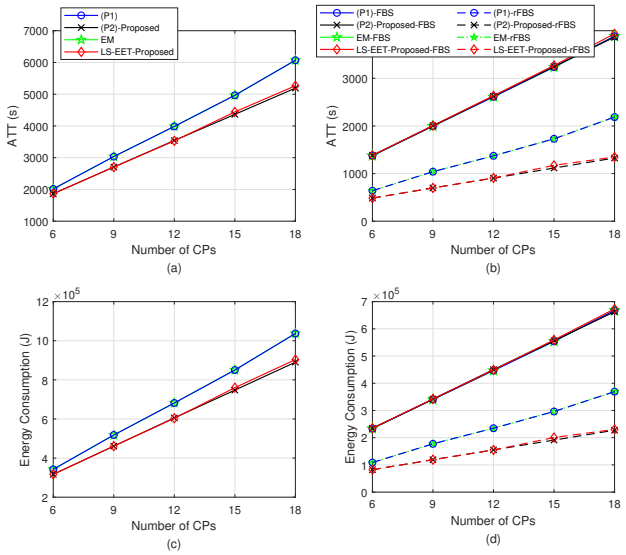

Fig. 3. ATT and energy consumption for all different schemes when $Q = 400$ Kbits.

the (P2) scheme and the LS-EET scheme generally achieve significant gains compared to both the (P1) and the EM schemes across all simulation scenarios whilst the (P1) and the EM schemes attain a comparable performance. Their performance is gradually increased as the N_V is increased compared to both the (P1) and the EM, and they gain approximately 14.5% when N_V=18, i.e., N_{out}=6 and N_{in}=12. Worth noticing that the LS-EET illustrates the performance compatible with the (P2) between N_V=6 and N_V=12 and then it is slightly increased after the case of N_V=12. In Fig. 3(b), the (P2) and the LS-EET generally gain better performance for the ATT$_u$ than both the (P1) and the EM, and they obtain up to 38.3% gain in the case of N_V=18.

Fig. 3(c) and (d) show the energy consumption in Joules (J) measured by the model in the section II-C for FBSs including both the FBS and the rFBS for all different schemes, and the energy consumption of the FBS and the rFBS respectively for all different schemes. We varied N_V composed of N_{out} and N_{in} in ratio of 1:2. As expected, the energy consumption of FBSs is shown similar linear aspect to the ATT. In Fig. 3(c), the (P2) and the LS-EET generally achieve great performance compared to both the (P1) and the EM in the entire simulations by gaining up to 14.1% in the case of $N_V = 18$. Moreover, in Fig. 3(d), the (P2) and the LS-EET also overall obtain better performance than the (P1) and the EM, and they attain up to 37.6% gain for the energy consumption of the rFBS in the case of $N_V = 18$. Furthermore, all schemes for the ATT$_k$ maintain similar performance.

V. Conclusions

This paper presents a novel optimization framework to allow for continuous service connectivity of flying base stations (FBSs) using aerial relay nodes with joint optimized trajectories to reduce the overall energy consumption and aggregated travel time (ATT). Furthermore, a proposed heuristic scheme allows for competitive decision making in real-time. A wide set of numerical investigations reveals that the proposed schemes provide significant gains in performance compared to previously defined nominal techniques where trajectories of FBSs, despite being optimal, are not jointly optimized. To this end, in terms of ATT compared to previous proposed techniques for the trajectory optimization, the average gain more than 14% for the entire fleet of FBSs is achieved, whilst for the relay FBS (rFBS), this average gain is more than 38%.

References

[1] N. Zhao, et al, "UAV-assisted emergency networks in disasters," *IEEE Wireless Communications*, Vol. 26, No. 1, pp 45-51, 2019.
[2] M. Mozaffari, et al, "A tutorial on UAVs for wireless networks: Applications, challenges, and open problems," *IEEE Communications Surveys & Tutorials*, Vol.21, No.3, pp 2334-2360, 2019.
[3] S. Zhang, et al, "Joint trajectory and power optimization for UAV relay networks," *IEEE Communications Letters*, Vol. 22, pp 161-164, 2017.
[4] B. Li, et al, "Joint Transmit Power and Trajectory Optimization for Two-Way Multi-Hop UAV Relaying Networks," *2020 IEEE International Conference on Communications Workshops* , IEEE, 2020.
[5] Q. Hu, et al, "Low-complexity joint resource allocation and trajectory design for UAV-aided relay networks with the segmented ray-tracing channel model," *IEEE Transactions on Wireless Communications*, Vol. 19, No. 9, pp 6179-6195, Sep 2020.
[6] X. Jiang, et al, "Trajectory and communication design for UAV-relayed wireless networks," *IEEE Wireless Communications Letters*, Vol. 8, No. 6, pp 1600-1603, Dec 2019.
[7] Q. Chen, "Joint Trajectory and Resource Optimization for UAV-Enabled Relaying Systems," *IEEE Access*, Vol. 8, pp 24108-24119, 2020.
[8] G. Zhang, et al, "Trajectory optimization and power allocation for multi-hop UAV relaying communications," *IEEE Access*, Vol. 6, 2018.
[9] B. Liu, Q. Zhu and H. Zhu, "Trajectory optimization and resource allocation for UAV-assisted relaying communications," *Wireless Networks*, Vol. 26, No. 1, pp 739-749, 2020.
[10] Z. Sun, et al, "Joint Energy and Trajectory Optimization for UAV-Enabled Relaying Network with Multi-Pair Users," *IEEE Transactions on Cognitive Communications and Networking*, Dec 2020.
[11] T. Kim and D. Qiao, "Energy-Efficient Data Collection for IoT Networks via Cooperative Multi-Hop UAV Networks,"*IEEE Transactions on Vehicular Technology*, Vol. 69, No. 11, pp 13796-13811, 2020.
[12] J. Miao, et al, "Secrecy Energy Efficiency Maximization for UAV Swarm Assisted Multi-Hop Relay System: Joint Trajectory Design and Power Control,"*IEEE Access*, Vol. 9, pp 37784-37799, 2021.
[13] C. H. Papadimitriou, "The Euclidean travelling salesman problem is NP-complete," *Theoretical computer science*, vol 4, no.3, pp 237-244, 1977.
[14] A. Al-Hourani, S. Kandeepan, and S. Lardner, "Optimal LAP altitude for maximum coverage," *IEEE Wireless Communications Letters,* Vol. 3, No. 6, pp569-572, 2014.
[15] M. Mozaffari, et al, "Unmanned aerial vehicle with underlaid device-to-device communications: Performance and tradeoffs,"*IEEE Transactions on Wireless Communications,* Vol. 15, No. 6, pp 3949-3963, Jun 2016.
[16] Y. Zeng, J. Xu and R. Zhang, "Energy minimization for wireless communication with rotary-wing UAV, " *IEEE Transactions on Wireless Communications*, Vol.18, No.4, pp2329-2345, 2019.
[17] Y. Zeng, X. Xu, and R. Zhang, "Trajectory design for completion time minimization in UAV-enabled multicasting," *IEEE Transactions on Wireless Communications*, Vol. 17, No. 4, pp. 2233–2246, Apr. 2018.
[18] J. Lee and V. Friderikos. "Path optimization for Flying Base Stations in Multi-Cell Networks, " *2020 IEEE Wireless Communications and Networking Conference (WCNC)*, IEEE, 2020.
[19] K. Dorling, et al, "Vehicle Routing Problems for Drone Delivery," *IEEE Transactions on Systems, Man, and Cybernetics: Systems*, vol. 47, no.1, pp 70-85, Jan 2017.
[20] Y. Xiao, et al, "Development of a fuel consumption optimization model for the capacitated vehicle routing problem,"*Computers & operations research*, Vol.39, No.7, pp 1419-1431, 2012.